ENVIRONMENTAL RESEARCH
LETTERS

LETTER • OPEN ACCESS

Stratospheric ozone loss-induced cloud effects lead to less surface ultraviolet radiation over the Siberian Arctic in spring

To cite this article: Yan Xia *et al* 2021 *Environ. Res. Lett.* **16** 084057

ENVIRONMENTAL RESEARCH
LETTERS

CrossMark

OPEN ACCESS

RECEIVED
18 May 2021

REVISED
21 July 2021

ACCEPTED FOR PUBLICATION
29 July 2021

PUBLISHED
5 August 2021

LETTER

Stratospheric ozone loss-induced cloud effects lead to less surface ultraviolet radiation over the Siberian Arctic in spring

Yan Xia[1,2], **Yongyun Hu**[3], **Yi Huang**[4], **Jianchun Bian**[2,5,6] **and Chuanfeng Zhao**[1,*]

[1] College of Global Change and Earth System Science, Beijing Normal University, Beijing 100875, People's Republic of China
[2] Key Laboratory of Middle Atmosphere and Global Environment Observation, Institute of Atmospheric Physics, Chinese Academy of Sciences, Beijing 100029, People's Republic of China
[3] Laboratory for Climate and Ocean-Atmosphere Studies, Department of Atmospheric and Oceanic Sciences, School of Physics, Peking University, 100871 Beijing, People's Republic of China
[4] Department of Atmospheric and Oceanic Sciences, McGill University, Montreal, Quebec H3A 0B9, Canada
[5] College of Earth and Planetary Sciences, University of Chinese Academy of Sciences, Beijing 100049, People's Republic of China
[6] College of Atmospheric Sciences, Lanzhou University, Lanzhou 730000, People's Republic of China
[*] Author to whom any correspondence should be addressed.

E-mail: czhao@bnu.edu.cn

Keywords: stratospheric ozone loss, the Siberian Arctic, ultraviolet radiation, high clouds, ERA5 reanalysis

Supplementary material for this article is available online

Abstract

Surface ultraviolet (UV) radiation has important effects on human health, terrestrial and aquatic ecosystems, and air pollution. Both stratospheric ozone and clouds are key factors that influence surface UV radiation. Here we find that Arctic ozone loss may lead to a decrease in surface UV radiation over the Siberian Arctic in spring using ERA5 reanalysis. It is found that Arctic ozone loss is associated with an increase in high clouds by modifying static stability in the upper troposphere. Stratospheric ozone loss allows more UV radiation to reach the surface. On the contrary, the increase in high clouds results in a reduction of surface UV radiation. Interestingly, a composite analysis suggests that this cloud masking effect is found to be stronger than that from stratospheric ozone loss over the Siberian Arctic in spring. These results suggest that we should pay more attention to the high-ozone events which would lead to more surface UV radiation by the cloud effects.

1. Introduction

The solar ultraviolet (UV) radiation reaching the Earth's surface is known to have pronounced impact on human health, agricultural productivity, terrestrial and aquatic ecosystems, and air quality (Douglass *et al* 2011 and Williamson *et al* 2014 and references therein). Stratospheric ozone effectively absorbs most of the solar UV radiation from about 200 to 315 nm in wavelength, which otherwise would potentially damage exposed life forms in the biosphere. Anthropogenic emission of ozone depleting substances (ODSs) results in ozone depletion in the global upper stratosphere and in the lower stratosphere in spring over both the Antarctic and Arctic (Solomon 1999, WMO 2018). Unlike the Antarctic ozone hole that develops annually during austral spring (September, October, and November), Arctic ozone levels usually stay well above the ozone hole threshold because of much stronger planetary wave activities in the Northern Hemisphere. It is found that the long-term stratospheric ozone depletion and associated increases in surface UV radiation have been successfully reduced by the implementation of the Montreal Protocol (Newman *et al* 2009, Mäder *et al* 2010, Dhomse *et al* 2018, WMO 2018). However, severe ozone loss still occurred over the Arctic in spring 2011 and 2020 associated with the anomalously strong and cold polar vortex (Hurwitz *et al* 2011, Manney *et al* 2011, 2020, Isaksen *et al* 2012, Myhre *et al* 2013, Dameris *et al* 2020, Hugelius *et al* 2020, Lawrence *et al* 2020), although ODSs have been declining since the late 1990s.

Furthermore, previous studies have demonstrated that surface UV radiation is also largely impacted by clouds as a result of scattering processes (Bais *et al* 1993, 2011, Calbó *et al* 2005, Watanabe *et al* 2011, López *et al* 2012, Williamson *et al* 2014). Indeed, changes in stratospheric ozone produce indirect effects in clouds as these changes modify the static stability in the upper troposphere and lower stratosphere due to changes in the vertical profile of temperatures especially over the Arctic and Antarctic (Xia *et al* 2016, 2018, 2020, 2021, Maleska *et al* 2020). It is found that an increase in high clouds is generally associated with stratospheric ozone depletion (Xia *et al* 2021). Because of the short wavelength of UV radiation, the increase in high clouds may have non-negligible masking effects and attenuate the surface UV radiation (Calbó *et al* 2005). On the contrary, stratospheric ozone depletion allows more UV radiation to reach the surface. These results raise an important question: how does surface UV radiation change resulting from both direct effects of stratospheric ozone depletion and indirect effects from accompanying increases in high clouds?

Xia *et al* (2021) found that Arctic ozone loss in March is likely shifted to central Siberia in April and May. The cloud effects associated with stratospheric ozone loss in spring 2020 play an important role in the abnormal surface warming in the Siberian Arctic. In this study, we do composition analysis to see how high clouds and surface UV radiation response to ozone loss in spring over the Siberian Arctic over 1979–2020 using ERA5 reanalysis. To better assess the role of high clouds, another analysis of low and middle clouds is also done. In the following sections, we will describe the data, method and the results in order.

2. Data and methods

2.1. Data

The monthly mean air temperature, cloud fraction, total column ozone, and downward UV radiation at the surface are from ERA5 reanalysis over 1979–2020. ERA5, which is the fifth generation ECMWF reanalysis for the global climate and weather, combines model data with observations from across the world into a globally complete and consistent dataset (Hersbach *et al* 2020). The datasets of temperature and cloud fraction have a horizontal resolution of 0.25° × 0.25° with 37 pressure levels from 1000 to 1 hPa. In ERA5 reanalysis, high clouds are defined as cloud cover occurring on model levels with a pressure less than 0.45 times the surface pressure. Downward UV radiation flux at surface is outputted as radiation with a wavelength of 200–440 nm since UV is essential for living organisms. The 1950–1978 period data from ERA5 has been released. However, we only investigate variations of surface UV radiation over 1979–2020 because severe ozone depletions mainly occurred after 1979 due to the anthropogenic emission of ODSs.

To confirm the impact of stratospheric ozone on high clouds, the monthly mean total column ozone from the multi sensor reanalysis version 2 (MSR-2) and the satellite observations of cloud fraction are also used here. The MSR-2 reanalysis, constructed using all available satellite observations, surface observations and a data assimilation technique using a chemistry transport model, has a horizontal resolution of 0.5° × 0.5° (van der A *et al* 2015a, 2015b). We use high clouds (cloud fraction above 400 hPa) from Clouds and the Earth's Radiant Energy System (CERES) Synoptic (SYN1deg) product. CERES SYN1deg provides monthly mean high clouds on a 1° × 1° grid over March 2000–May 2020 (Doelling *et al* 2013, 2016, Rutan *et al* 2015).

2.2. Method

We use composite analysis to analyze the impact of ozone loss on surface UV radiation in spring over the Siberian Arctic. The composite analysis is widely used in climate studies (Xie *et al* 2017, 2020). Following Xia *et al* (2021), we define the Siberian ozone (SO) index as the area-weighted spatial-mean total ozone over 60°–80° N and 60°–120° E to composite the anomalies of both ozone and surface UV radiation. Linear trends and averages over 1979–2020 are removed because we mainly focus on the interannual variability. The composite anomalies are computed by the difference between the low (high) ozone events and climatological mean over 1979–2020. We define the low (high) ozone events as years with the SO index of less (greater) than minus (plus) one standard deviation for each month (figure S1 (available online at stacks.iop.org/ERL/16/084057/mmedia)). The low- and high-ozone years are listed in table S1. There are 7 low-ozone years for all the three months. The numbers of high-ozone years are 7, 4, and 5 in March, April, and May, respectively. The statistical significance of the composite anomalies is assessed by the Student's *t*-test.

3. Results

It is found that the composite ozone anomalies for the low-ozone events are characterized by significant ozone depletion over the Arctic in March which is shifted toward the Siberian Arctic in April and May (figures S2(a)–(c)). The ozone depletions averaged over the Siberian Arctic are about 55, 63, and 23 Dobson Units (DU) in March, April, and May, respectively. The high-ozone events feature predominant increases in ozone centered over the Siberian Arctic with average values of about 48, 44, and 23 DU in March, April, and May, respectively (figures S2(d)–(f)).

Figures 1(a)–(c) show the correlation coefficients between the SO index and high clouds over 1979–2020 in ERA5 reanalysis. It indicates that the SO index is negatively correlated with high clouds over the Siberian Arctic in March (figure 1(a)). The minimum of the correlation coefficients is about −0.61. The negative correlation coefficients in April are mainly located over the western half of the Siberian Arctic (60°–90° E), which can reach about −0.65 (figure 1(b)). In May, both the magnitude (−0.46)

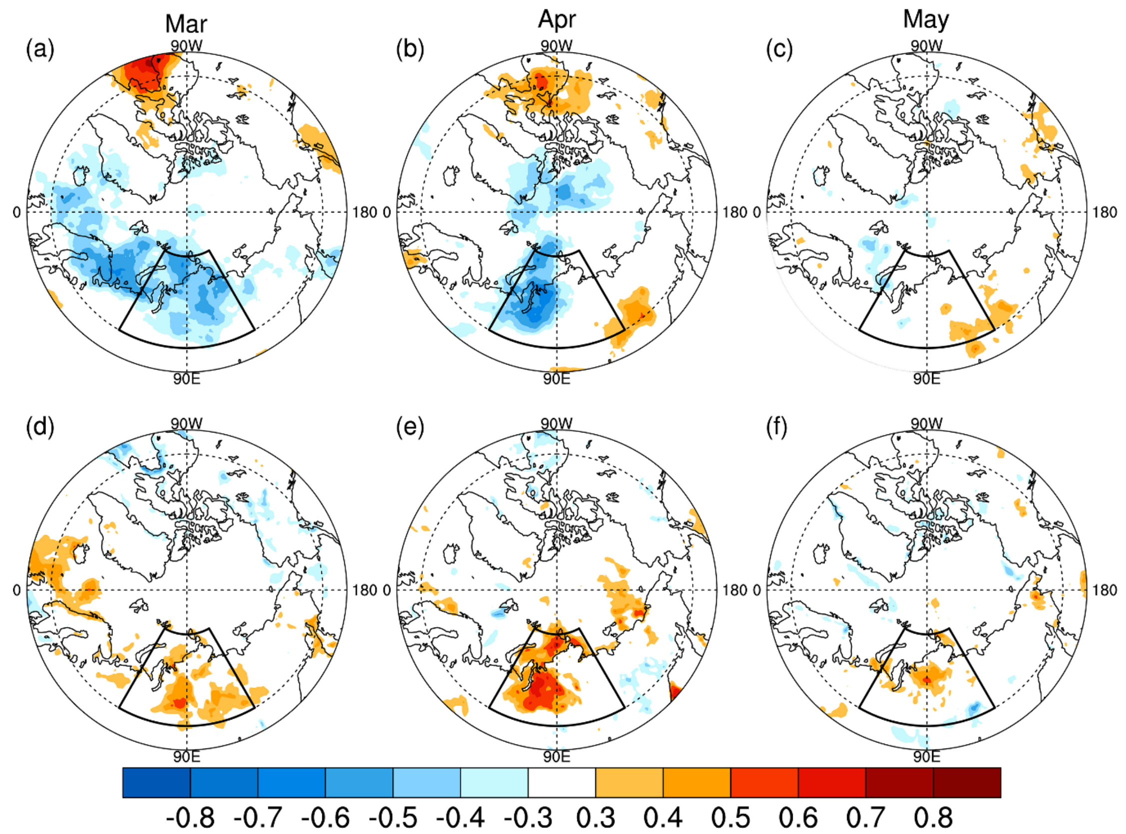

Figure 1. Geographic distributions of the correlation coefficients between the SO index and (a)–(c) high clouds and (d)–(f) downward surface UV radiation over 1979–2020 in March, April, and May based on ERA5 reanalysis. Box blacks indicate the concerned Arctic Siberian region over 60°–80° N and 60°–120° E. The correlation coefficient of ±0.3 corresponds to the 95% confidence level for the 42 years.

and area of the negative correlation coefficients are the smallest over the Siberian Arctic, which may be caused by the weakest interannual variability of the stratospheric ozone (figure S1). Figure S3 shows the correlation coefficients between the SO index from MSR-2 and high clouds from CERES SYN1deg over 2000–2020. It is highly consistent with the results in ERA5 reanalysis over the Arctic. The results indicate that high clouds are highly correlated with stratospheric ozone over the Siberian Arctic especially in March and April, which is consistent with previous work (Maleska *et al* 2020, Xia *et al* 2021). Our analysis indicates that the anti-correlation between the SO index and high clouds in North Canada is likely caused by the large-scale circulation (the Arctic oscillation) over the Arctic.

As mentioned above, both ozone and clouds can affect the downward UV radiation at surface. The correlation coefficients between the SO index and surface UV radiation over 1979–2020 are shown in figures 1(d)–(f). Interestingly, surface UV radiation in the Siberian Arctic is positively correlated with the SO index in March, April, and May, with maximum values of about 0.63, 0.69, and 0.59, respectively. This means that indirect effects on high clouds derived from ozone loss over the Siberian Arctic may result in a reduction of surface UV radiation. The positive correlation coefficients in March are mainly located over the southern half of the Siberian Arctic (60°–70° N), which may be primarily due to the less solar radiation poleward of 70° N in March (figure 1(d)). The spatial distribution in April suggests a strong connection between stratospheric ozone and surface UV radiation over the western half of the Siberian Arctic (figure 1(e)), which is highly consistent with that between the SO index and high clouds (figure 1(b)). In May, the weak positive correlation coefficients have the smallest magnitude and area (figure 1(f)), which is also similar to the high clouds (figure 1(c)).

Figure 2 shows the vertical cross-section of composite anomalies of temperature and cloud averaged over 60°–120° E for the low-ozone events in March, April, and May. We find that significant stratospheric cooling, which is mainly located north of 60° N above 300 hPa, is associated with the ozone depletion in March, April, and May, which is consistent with previous findings (Randel *et al* 2009, Checa-Garcia *et al* 2018). The cooling anomalies increase with increasing altitude and are the weakest in May because of the smallest ozone loss. The warm anomalies in the troposphere, which are also related to the ozone depletion, are the strongest in April, which is consistent with the results in Xia *et al* (2021). The stratospheric cooling leads to an enhancement of the vertical temperature lapse rate at the tropopause region

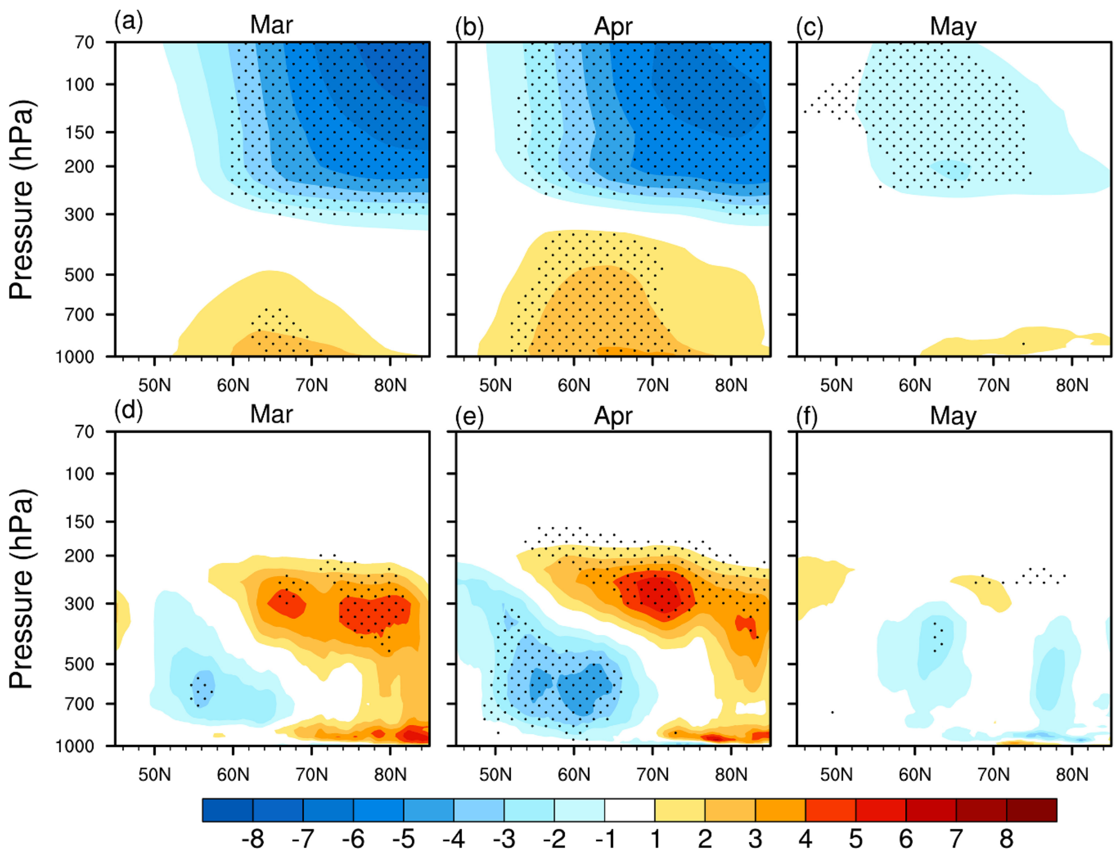

Figure 2. Vertical cross-section of composite anomalies of (a)–(c) temperature and (d)–(f) cloud averaged over 60°–120° E for the low-ozone events in March, April, and May based on ERA5 reanalysis. The unit of panels (a)–(c) is K and then (d)–(f) is %, and they share the same colormap. Regions with dots are the places where regressions have statistical significance levels higher than the 95% confidence level based on the Student's *t*-test.

and consequent decreases of static stability in the upper troposphere. The decreases in static stability further result in an increase of high clouds located north of 60° N between 400 and 200 hPa especially in March and April with maximum values of about 5.9% and 6.6%, respectively (figures 2(d)–(f)). Furthermore, significant decreases in middle and low clouds occur between 50° N and 65° N below 400 hPa especially in April, which may be caused by the decrease of the meridional temperature gradient in the lower troposphere and consequent reduction of mid-latitude cyclones. Because of the weaker magnitude of the ozone anomalies for the high-ozone events (figure S2), the responses of stratospheric temperature and high clouds are much weaker than those for the low-ozone events especially in April and May (figure S4). The composite anomalies for high-ozone events show consistent results that an increase in ozone leads to a stratospheric warming and thus a reduction of high clouds above 400 hPa.

Figure 3 shows the composite anomalies of high clouds for the low-ozone events and the high-ozone events over the Siberian Arctic in March, April, and May. The climatological spatial pattern shows that the Siberian Arctic is covered by plenty of high clouds with a maximum value of about 47.4% in spring (figures S5(a)–(c)), which is consistent with the results in Chernokulsky and Esau (2019). In March, the high clouds increase throughout the Siberian Arctic with a maximum of about 9.0% for the low-ozone case (figure 3(a)). Similarly, a significant decrease of high clouds is associated with the high-ozone case (figure 3(d)). The center of this reduction, which can reach about −11.4%, is mainly located over the southern half of the Siberian Arctic, which is likely due to the spatial inhomogeneity of the high-clouds climatology (figure S5(a)). In April, the increase of high clouds for the low-ozone events is mainly located over the western part of the Siberian Arctic including the Kara Sea and the adjacent coastal region (figure 3(b)). The maximum values of this increase are larger than 11.7%, and the change in high clouds averaged over 60°–80° N and 60°–90° E is about 6.2%. We find consistent results for the high-ozone events that a decrease of high clouds is mainly located over the western part of the Siberian Arctic in the coastal regions close to the Kara Sea, with a minimum value of about −11.4% and an average value of about −5.6% (figure 3(e)). The spatial distribution of the composite anomalies in May generally shows a dipole pattern over the Siberia with a northwest–southeast tilt (figures 3(c) and (f)). The increases/decreases of high clouds associated with the low/high-ozone events, which can reach about 6.2%/−7.8%,

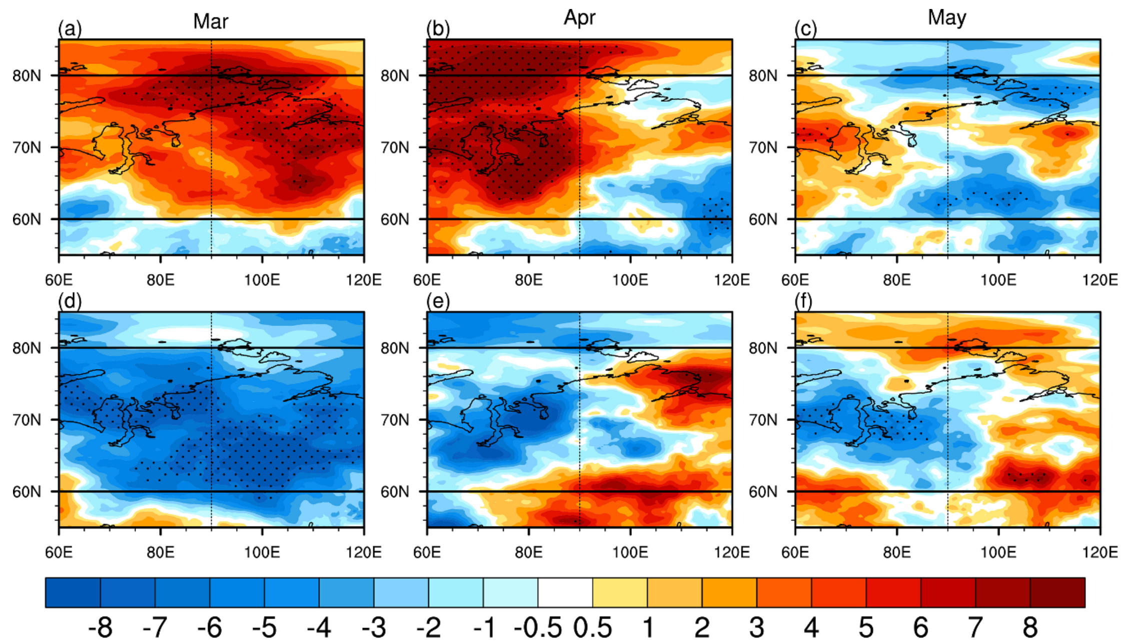

Figure 3. Geographic distributions of composite anomalies of high clouds for (a)–(c) the low-ozone events and (d)–(f) the high-ozone events in March, April, and May (unit: %) based on ERA5 reanalysis. Regions with dots are the places where regressions have statistical significance levels higher than the 95% confidence level.

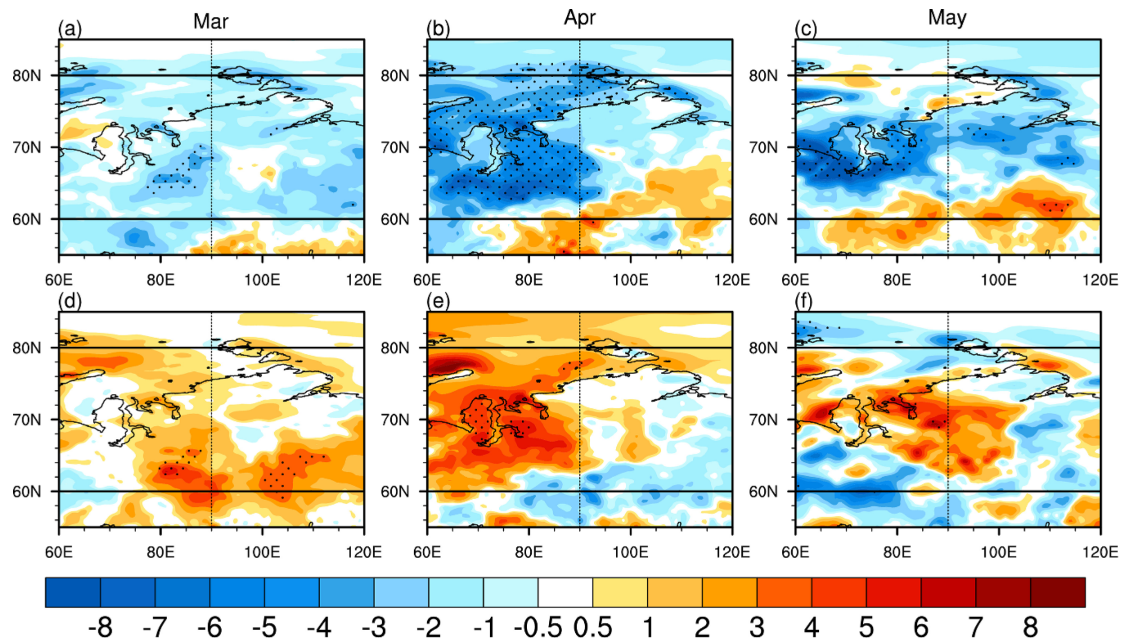

Figure 4. Geographic distributions of the ratios between composite anomalies of surface UV radiation and the climatological mean over 1979–2020 for (a)–(c) the low-ozone events and (d)–(f) the high-ozone events in March, April, and May (unit: %) based on ERA5 reanalysis. Regions with dots are the places where regressions have statistical significance levels higher than the 95% confidence level.

are mainly located in the coastal regions near the Kara Sea, which is similar to those in April but has a smaller magnitude. The dipole pattern with both positive and negative anomalies largely reduces the zonal mean changes in high clouds shown in figure 2(f).

Figure 4 shows the ratios between the composite anomalies of surface UV radiation and the climatological mean over 1979–2020 for the low-ozone events and the high-ozone events in March, April, and May. It is found that the changes in clouds associated with the ozone changes play a primary role in variations of downward UV radiation at surface. In March, the increase in high clouds leads to a reduction of surface UV radiation over the Siberian Arctic with a maximum of about 4.6% for the low-ozone case (figure 4(a)). Interestingly, the southward displacement of the decrease of high clouds results in an increase in surface UV radiation centered at around 63° N for the high-ozone events (figure 4(d)). The percentage increase of surface UV radiation can reach about 6.1% at regions where the climatological mean is about 12 W m^{-2} (figure S5(d)). In April, the decrease/increase in surface UV radiation shows high spatial consistency with the increase/decrease in high clouds for low/high-ozone case (figures 4(b) and (e)). The increase of high clouds over the Kara Sea and adjacent coastal regions causes a local decrease of surface UV radiation for the low-ozone case (figure 4(b)). Similarly, both a decrease of high clouds and an increase of surface UV radiation occur over the coastal regions close to the Kara Sea for the high-ozone events (figure 4(e)). Both the maximum decreases and increases in surface UV radiation are larger than 9.0% in April over the coastal regions where the climatological UV radiation at surface is more than 19 W m^{-2} (figure S5(e)). We note that the climatology of surface UV radiation is larger in the Arctic Ocean and coastal regions (more than 25 W m^{-2}) than that at lower latitudes (figure S5(f)). It is found that ozone loss favors less downward UV radiation at surface near the coastal regions at around 70° N in May (figure 4(c)) while high-ozone events favor more surface UV radiation at the center of the Siberian Arctic (figure 4(f)). The maximum percent decrease and increase of surface UV radiation can reach about 13.7% and 7.4% for the low-ozone and high-ozone events, respectively.

To check the effects of low and middle clouds, the correlation coefficients between the SO index and total, middle, and low clouds are also investigated (figure S6). It is found that the SO index is not significantly correlated with the local middle and low clouds. Ozone in the Siberian Arctic is related to the clouds in the mid-latitudes in March (figures 1(a) and S6(a), (d), and (g)), which may be due to the influence of the large-scale circulation such as Arctic oscillation. In April and May, the SO index is linked to the middle and low clouds located to the south of the Siberian Arctic (figures S6(e)–(f) and (h)–(i)), which may result from the reduction of mid-latitude cyclones caused by the decrease of the meridional temperature in the troposphere (figures 2(a)–(c)).

4. Conclusions and discussions

Both the correlation and composite analyses show that ozone depletion favors a reduction of downward UV radiation at surface over the Siberian Arctic in spring. We find that this reduction of surface UV radiation is mainly caused by the increase in high clouds associated with ozone depletion. Stratospheric ozone loss cools the stratosphere in spring and leads to a consequent decrease of static stability in the upper troposphere which further results in more local high clouds. The composite analysis indicates that the largest decreases in surface UV radiation for the low-ozone events can reach about 4.6%, 9.1%, and 13.7% in March, April, and May, respectively. Similarly, the high-ozone events favor maximum increases of surface UV radiation by about 6.1%, 10.2%, and 7.4% in March, April, and May, respectively.

We find that the responses of high clouds and surface UV radiation show high spatial inhomogeneity. The reduction of surface UV radiation associated with ozone depletion mainly occurs in the southern, western, and central parts of the Siberian Arctic in March, April, and May, respectively. The increase of surface UV radiation for the high-ozone events has similar spatial patterns. It is interesting to note that an increase of surface UV radiation occurs to the south of the negative anomaly in April and May for the low-ozone events. This may be caused by the reduction of low and middle clouds located southward of 65° N (figures 2(e) and (f)).

In this study, the changes in high clouds caused by stratospheric ozone loss-induced cooling are highlighted. However, we should note that stratospheric temperature can also be impacted by the radiative effects of clouds and stratospheric water vapor, convections, and surface temperature (Ceppi *et al* 2017). We find that the lower-stratospheric temperatures are highly correlated with ozone over the Siberian Arctic with a maximum value of about 0.85 (figure S7). The positive correlation coefficients are much smaller in other regions than those in the Siberian Arctic because of the largest variations of ozone there (figures S7 and S8). This spatial inhomogeneity further influences the relationship between ozone and high clouds and surface UV. The polar cap is subdivided into six segments (0°–60° E, 60°–120° E, 120°–180° E, 180°–120° W, 120°–60° W, and 60°–0° W). Figures S9–14 show the correlation coefficients between the ozone index averaged over each segment and high clouds and downward surface UV radiation over 1979–2020 in March, April, and May. It is found that our hypothesis that low ozone correlates with low UV is only valid in the Siberian Arctic (60°–120° E) in April and May. In March, this result can also be seen over 0°–60° E, 120°–180° E, and 60°–0° W (figures S9, S11, and S14) where high correlation coefficients between lower-stratospheric temperature and ozone occur (figure S7(a)).

It is important to note that Arctic ozone depletion leads to more downward UV radiation at the surface for clear-sky condition especially at noon time (Neale *et al* 2021). Here, we focus on the monthly mean surface UV radiation which also has important effects on the ecosystems and is largely affected by clouds. Our results suggest that we should pay more attention to the high-ozone events which may lead to more surface UV radiation by the cloud effects over the Siberian Arctic.

Data availability statement

The data that support the findings of this study are openly available at the following URL/DOI: https://cds.climate.copernicus.eu/cdsapp#!/search?type=dataset%26;text=ERA5 for the ERA5 reanalysis. The MSR-2 reanalyisis of the total column ozone can be found at www.temis.nl/protocols/O3global.html. The CERES SYN1deg observations of cloud fraction are available at https://ceres-tool.larc.nasa.gov/ord-tool/jsp/SYN1degEd41Selection.jsp.

Acknowledgments

We thank Dr Jian Yue for helpful comments. This work is supported by the Second Tibetan Plateau Scientific Expedition and Research Program (STEP), under Grant of 2019QZKK0604, Key Laboratory of Middle Atmosphere and Global environment Observation (LAGEO-2020-09), and the Fundamental Research Funds for the Central Universities. C Zhao is supported by the National Natural Science Foundation of China (NSFC), under Grants 41925022 and 91837204. Y Hu is supported by the National Natural Science Foundation of China (NSFC), under Grant 41761144072.

ORCID iDs

Yan Xia https://orcid.org/0000-0001-8664-5325
Chuanfeng Zhao https://orcid.org/0000-0002-5196-3996

References

Bais A F *et al* 2011 Projections of UV radiation changes in the 21st century: impact of ozone recovery and cloud effects *Atmos. Chem. Phys.* **11** 7533–45

Bais A F, Zerefos C S, Meleti C, Ziomas I C and Tourpali K 1993 Spectral measurements of solar UVB radiation and its relations to total ozone, SO_2, and clouds *J. Geophys. Res. Atmos.* **98** 5199–204

Calbó J, Pagès D and González J-A 2005 Empirical studies of cloud effects on UV radiation: a review *Rev. Geophys.* **43** RG2002

Ceppi P, Brient F, Zelinka M D and Hartmann D L 2017 Cloud feedback mechanisms and their representation in global climate models *WIREs Clim. Change* **8** e465

Checa-Garcia R, Hegglin M I, Kinnison D, Plummer D A and Shine K P 2018 Historical tropospheric and stratospheric ozone radiative forcing using the CMIP6 database *Geophys. Res. Lett.* **45** 3264–73

Chernokulsky A and Esau I 2019 Cloud cover and cloud types in the Eurasian Arctic in 1936–2012 *Int. J. Climatol.* **39** 5771–90

Dameris M, Loyola D G, Nützel M, Coldewey-Egbers M, Lerot C, Romahn F and van Roozendael M 2020 First description and classification of the ozone hole over the Arctic in boreal spring 2020 *Atmos. Chem. Phys.* **2021** 1–26

Dhomse S S *et al* 2018 Estimates of ozone return dates from chemistry-climate model initiative simulations *Atmos. Chem. Phys.* **18** 8409–38

Doelling D R, Loeb N G, Keyes D F, Nordeen M L, Morstad D, Nguyen C, Wielicki B A, Young D F and Sun M 2013 Geostationary enhanced temporal interpolation for CERES flux products *J. Atmos. Ocean. Technol.* **30** 1072–90

Doelling D R, Sun M, Nguyen L T, Nordeen M L, Haney C O, Keyes D F and Mlynczak P E 2016 Advances in geostationary-derived longwave fluxes for the CERES synoptic (SYN1deg) product *J. Atmos. Ocean. Technol.* **33** 503–21

Douglass A *et al* 2011 Stratospheric ozone and surface ultraviolet radiation, chapter 2 in scientific assessment of ozone depletion: 2010 *Global Ozone Research and Monitoring Project–Report No. 52* (World Meteorological Organization)

Hersbach H *et al* 2020 The ERA5 global reanalysis *Q. J. R. Meteorol. Soc.* **146** 1999–2049

Hugelius G *et al* 2020 Large stocks of peatland carbon and nitrogen are vulnerable to permafrost thaw *Proc. Natl Acad. Sci.* **117** 20438–46

Hurwitz M M, Newman P A and Garfinkel C I 2011 The Arctic vortex in March 2011: a dynamical perspective *Atmos. Chem. Phys.* **11** 11447–53

Isaksen I S A *et al* 2012 Attribution of the Arctic ozone column deficit in March 2011 *Geophys. Res. Lett.* **39** L24810

Lawrence Z D, Perlwitz J, Butler A H, Manney G L, Newman P A, Lee S H and Nash E R 2020 The remarkably strong Arctic stratospheric polar vortex of winter 2020: links to record-breaking Arctic oscillation and ozone loss *J. Geophys. Res. Atmos.* **125** e2020JD033271

López M L, Palancar G G, Toselli B M and Transfer R 2012 Effects of stratocumulus, cumulus, and cirrus clouds on the UV-B diffuse to global ratio: experimental and modeling results *J. Quant. Spectrosc. Radiat. Transfer* **113** 461–9

Mäder J A, Staehelin J, Peter T, Brunner D, Rieder H E and Stahel W A 2010 Evidence for the effectiveness of the Montreal Protocol to protect the ozone layer *Atmos. Chem. Phys.* **10** 12161–71

Maleska S, Smith K and Virgin J 2020 Impacts of stratospheric ozone extremes on Arctic high cloud *J. Clim.* **33** 1–41

Manney G L *et al* 2011 Unprecedented Arctic ozone loss in 2011 *Nature* **478** 469–75

Manney G L *et al* 2020 Record-low Arctic stratospheric ozone in 2020: MLS observations of chemical processes and comparisons with previous extreme winters *Geophys. Res. Lett.* **47** e2020GL089063

Myhre G *et al* 2013 Anthropogenic and natural radiative forcing *Climate Change 2013: The Physical Science Basis. Contribution of Working Group I to the Fifth Assessment Report of the Intergovernmental Panel on Climate Change* ed T F Stocker *et al* (Cambridge: Cambridge University Press) pp 659–740

Neale R E *et al* 2021 Environmental effects of stratospheric ozone depletion, UV radiation, and interactions with climate change: UNEP Environmental Effects Assessment Panel, update 2020 *Photochem. Photobiol. Sci.* **20** 1–67

Newman P A *et al* 2009 What would have happened to the ozone layer if chlorofluorocarbons (CFCs) had not been regulated? *Atmos. Chem. Phys.* **9** 2113–28

Randel W J *et al* 2009 An update of observed stratospheric temperature trends *J. Geophys. Res. Atmos.* **114** 2107

Rutan D A, Kato S, Doelling D R, Rose F G, Nguyen L T, Caldwell T E and Loeb N G 2015 CERES synoptic product: methodology and validation of surface radiant flux *J. Atmos. Ocean. Technol.* **32** 1121–43

Solomon S 1999 Stratospheric ozone depletion: a review of concepts and history *Rev. Geophys.* **37** 275–316

van der A R J, Allaart R, M and Eskes H 2015a Multi-sensor reanalysis (MSR) of total ozone, version 2 *Royal Netherlands Meteorological Institute (KNMI)* (https://www.temis.nl/protocols/O3global.php and https://10.21944/temis-ozone-msr2)

van der A R J, Allaart R, M and Eskes H 2015b Extended and refined multi sensor reanalysis of total ozone for the period 1970–2012 *Atmos. Meas. Tech.* **8** 3021–35

Watanabe S, Sudo K, Nagashima T, Takemura T, Kawase H and Nozawa T 2011 Future projections of surface

UV-B in a changing climate *J. Geophys. Res.* **116** D16118

Williamson C E *et al* 2014 Solar ultraviolet radiation in a changing climate *Nat. Clim. Change* **4** 434–41

WMO (World Meteorological Organization) 2018 Scientific assessment of ozone depletion: 2018 *Global Ozone Research and Monitoring Project–Report No. 58* Geneva, Switzerland p 588

Xia Y, Hu Y and Huang Y 2016 Strong modification of stratospheric ozone forcing by cloud and sea-ice adjustments *Atmos. Chem. Phys.* **16** 7559–67

Xia Y, Hu Y, Huang Y, Zhao C, Xie F and Yang Y 2021 Significant contribution of severe ozone loss to the Siberian-Arctic surface warming in spring 2020 *Geophys. Res. Lett.* **48** e2021GL092509

Xia Y, Hu Y, Liu J, Huang Y, Xie F and Lin J 2020 Stratospheric ozone-induced cloud radiative effects on Antarctic sea ice *Adv. Atmos. Sci.* **37** 505–14

Xia Y, Huang Y and Hu Y 2018 On the climate impacts of upper tropospheric and lower stratospheric ozone *J. Geophys. Res. Atmos.* **123** 730–9

Xie F, Li J, Zhang J, Tian W, Hu Y, Zhao S, Sun C, Ding R, Feng J and Yang Y 2017 Variations in North Pacific sea surface temperature caused by Arctic stratospheric ozone anomalies *Environ. Res. Lett.* **12** 114023

Xie F, Zhang J, Li X, Li J, Wang T and Xu M 2020 Independent and joint influences of eastern Pacific El Niño–southern oscillation and quasi-biennial oscillation on Northern Hemispheric stratospheric ozone *Int. J. Climatol.* **40** 5289–307